

Global sensitivity analysis for statistical model parameters

Joseph Hart¹, Julie Bessac², and Emil Constantinescu^{2,3}

¹Department of Mathematics, North Carolina State University, Raleigh, NC

²Mathematics and Computer Science Division, Argonne National Laboratory, Lemont, IL

³The University of Chicago, Chicago, IL

Abstract

Global sensitivity analysis (GSA) is frequently used to analyze the influence of uncertain parameters in mathematical models. In principle, tools from GSA may be extended to analyze the influence of parameters in statistical models. Such analyses may enable parsimonious modeling and greater predictive capability. However, difficulties such as parameter correlation, model stochasticity, and multivariate model output prohibit a direct extension of GSA tools to statistical models. We introduce a novel framework that addresses these difficulties and enables GSA for statistical model parameters. Theoretical and computational properties are considered and illustrated on a synthetic example. The framework is applied to a Gaussian process model that depends on 95 parameters from the literature. Non-influential parameters are discovered through GSA and a reduced model with equal or stronger predictive capability is constructed by using only 79 parameters.

1 Introduction

Global sensitivity analysis (GSA) aims to quantify the relative importance of input variables or factors in determining the value of a function [1]; the traditional framework focuses on real-valued deterministic functions $f : \mathbb{R}^n \rightarrow \mathbb{R}$. Two common ways to measure contributions from the inputs are variance-based [2–4] and derivative-based methods [5–8]. Variance-based methods have richer theoretical foundations and do not require that f be differentiable. Derivative-based methods have less theoretical development; however, they have been observed to yield similar results and may be computed more efficiently. The Morris method [9] is another commonly used tool from GSA which is related to derivative-based methods. It computes elementary effects using only function evaluations and gains efficiency through experimental design.

In this paper we propose a derivative-based strategy for GSA of statistical models. GSA has been used widely for analysis of parameter uncertainty in mathematical models [1, 10]. In particular, GSA may be used to improve modeling insight, encourage model

parsimony, and accelerate the model-fitting process. To our knowledge, the GSA tools developed for mathematical models have not been systematically developed for analysis of statistical models. In particular, the combination of correlated inputs, model stochasticity, multivariate model output, and having an unknown parameter distribution prohibits a direct application of GSA tools to statistical models. Nevertheless, problem structure in statistical models may be exploited to enable efficient GSA. This paper provides a framework to use existing GSA tools in mathematics along with tools from statistics to address these challenges and yield a powerful new GSA tool for analysis of statistical models.

This work is motivated by a statistical model that fuses two datasets of atmospheric wind speed in order to provide statistical prediction of wind speed in space and time [11]. The predictions are generated from a Gaussian process whose mean and covariance are parameterized through a large number of parameters. Our objective in this application is to reduce the dimension of the parameter space making the model easier to fit and interpret. The GSA method is developed in an abstract setting and subsequently used to analyze this Gaussian process model.

To perform GSA, a probability distribution must be defined on the input space, and the analysis is done with respect to it. GSA has been well developed and studied for problems where the inputs are independent. In many statistical models, however the inputs (parameters) are correlated, thus posing additional challenges to traditional GSA tools. Developing GSA tools for problems with correlated inputs is an active area of research [12–21]. In addition to the theoretical and computational challenges posed by input correlations, simply defining or fitting a joint distribution on the inputs may be challenging in the context of statistical models.

To perform GSA on statistical models, we face one additional hurdle. A space-time Gaussian process, as in our motivating application, is not a deterministic real-valued function but rather a stochastic vector-valued function. Real-valued stochastic processes are considered in [22] and vector-valued deterministic models in [23]; generalizing GSA tools to stochastic or vector-valued functions is also an active area of research.

This article provides a framework to connect the mathematical and statistical tools needed to extend GSA to statistical models. We use a loss function for the statistical model in order to define a joint probability distribution that respects the correlation structure in the problem. This distribution is sampled by using a Markov Chain Monte Carlo method, and derivative-based sensitivity indices are computed from these samples. In this framework, we are able to discover both sensitivities and correlation structures without requiring a priori knowledge about the model.

We provide definitions and construct the abstract framework in Section 2. Section 3 details the computational methodology and summarizes the proposed method. In Section 4, we present numerical results for a synthetic test problem and for our motivating application. Section 5 provides a brief summary of our conclusions.

2 Preliminaries

Let \mathcal{G} be a statistical model defined through parameters $\theta = (\theta_1, \theta_2, \dots, \theta_n)^T \in A$, $A \subseteq \mathbb{R}^n$. Let $\mathcal{L} : A \rightarrow \mathbb{R}$ be a loss function associated with \mathcal{G} ; that is, to fit \mathcal{G} to data, one computes $\arg \min_{\theta \in A} \mathcal{L}(\theta)$. For instance, \mathcal{G} may be a Gaussian process with mean $\mu(\theta)$ and covariance $\Sigma(\theta)$; both depend on a vector of parameters θ . \mathcal{L} is the negative log likelihood.

We are interested in the global sensitivity of \mathcal{G} with respect to θ . Since \mathcal{G} may be a complex mathematical object, we propose to analyze the global sensitivity of \mathcal{G} to θ through the global sensitivity of \mathcal{L} to θ . This is appropriate since \mathcal{L} encodes the dependence of \mathcal{G} on θ . Further, since \mathcal{L} is a deterministic real-valued function of θ , it is significantly easier to analyze than \mathcal{G} . In general \mathcal{G} may be a stochastic vector-valued function of θ .

One challenge is that the statistical model \mathcal{G} may be mathematically well defined for parameters $\theta \in A$ but yield a practically irrelevant solution in the context of a given application. To avoid this scenario, we let $B \subseteq A$ be the subset that restricts A to parameters yielding relevant solutions. For instance, a quantity in \mathcal{G} may be required to be nonnegative so B restricts to parameters respecting this constraint. We assume that B is a Lebesgue measurable set; this is easily verified in most applications.

We make three assumptions about \mathcal{L} ; formally, they are expressed as the following.

I \mathcal{L} is differentiable.

II $\exists \delta_{\min} \geq 0$ such that $\int_B e^{-\delta_{\min} \mathcal{L}(\theta)} d\theta$, $\int_B |\theta_k| e^{-\delta_{\min} \mathcal{L}(\theta)} d\theta$, and $\int_B |\frac{\partial \mathcal{L}}{\partial \theta_k}(\theta)| e^{-\delta_{\min} \mathcal{L}(\theta)} d\theta$, $k = 1, 2, \dots, n$, exist and are finite.

III $\exists L_{\min} \in \mathbb{R}$ such that $L_{\min} \leq \mathcal{L}(\theta)$, $\forall \theta \in B$.

Assumption I is necessary since we seek to use a derivative-based GSA. This assumption is easily verifiable in most cases. Assumption II is needed so that global sensitivity indices (3) are well defined. Assumption III is a needed technical assumption requiring that the loss function be bounded below. Note that if \mathcal{L} is continuously differentiable and B is compact, then all three assumptions follow immediately; this is a common case.

To define global sensitivity indices, we must specify a probability measure to integrate against. Let

$$q(\theta) = \chi_B(\theta) e^{-\delta(\mathcal{L}(\theta) + \lambda \|\theta\|_2^2)} \quad (1)$$

for some $\delta \geq \delta_{\min}$ and $\lambda \geq 0$; χ is the characteristic function of a set, and $\|\cdot\|_2$ is the Euclidean norm. Note that B is defined through constraints on \mathcal{G} so it is generally difficult to express B in terms of simple algebraic constraints. In most cases, however, the constraints may be checked when \mathcal{L} is evaluated, and hence q is easily evaluated through evaluating \mathcal{L} .

From Assumption II and the fact that $e^{-\delta \lambda \|\theta\|_2^2} \leq 1$, it follows that q is integrable. We define the probability density function (PDF) as

$$p(\theta) = \frac{q(\theta)}{\int_A q(\gamma) d\gamma} = \frac{e^{-\delta(\mathcal{L}(\theta) + \lambda \|\theta\|_2^2)}}{\int_B e^{-\delta(\mathcal{L}(\gamma) + \lambda \|\gamma\|_2^2)} d\gamma}. \quad (2)$$

Then p is supported on B and gives the greatest probability to regions where \mathcal{L} is close to its minimum namely, where θ is a good fit. A PDF of this form corresponds to a Gibbs measure [24] with temperature δ ; the temperature determines how the probability mass disperses from the modes. The scalar $\lambda \geq 0$ is a regularization factor that aids when p is too heavy tailed; this is illustrated in Section 4. The determination of δ and λ is considered in Section 3. Note that determining a PDF for correlated parameters may be challenging in general. This framework provides a natural way to define the PDF, but it comes at the cost of needing to determine δ and λ .

Definition 1. Let the sensitivity index of \mathcal{G} with respect to θ_k be defined as

$$S_k = \mathbb{E}(|\theta_k|) \mathbb{E}\left(\left|\frac{\partial \mathcal{L}}{\partial \theta_k}(\theta)\right|\right) = \int_B |\theta_k| p(\theta) d\theta \int_B \left|\frac{\partial \mathcal{L}}{\partial \theta_k}(\theta)\right| p(\theta) d\theta. \quad (3)$$

The reasoning behind (3) is that the expected partial derivative, $\mathbb{E}\left(\left|\frac{\partial \mathcal{L}}{\partial \theta_k}(\theta)\right|\right)$, is a measure of global sensitivity that depends on the units of θ_k . This dependence may create challenges because parameters on multiple scales are difficult to compare. Scaling by $\mathbb{E}(|\theta_k|)$ alleviates this problem, yielding scale-invariant global sensitivity indices. For the subsequent development we assume that the gradient $\nabla \mathcal{L}$ is available; finite-difference approximations may be used otherwise.

Correlations in θ make Monte Carlo integration with uniform sampling intractable for computing the S_k 's. Importance sampling may be used if an efficient proposal distribution is found; however, this is also challenging in most cases. Therefore, we propose to compute the S_k 's with Markov Chain Monte Carlo (MCMC) methods.

In summary, the global sensitivity of \mathcal{G} to θ may be estimated by using only evaluations of \mathcal{L} and $\nabla \mathcal{L}$ along with MCMC. This framework also admits additional useful information as by-products of estimating (3). More details are given in Section 3.

3 Computing sensitivities

In this section we present the main result of this study. The proposed method may be partitioned into three stages:

- i Preprocessing where we collect information about the loss function,
- ii Sampling where samples are drawn from the probability measure (2),
- iii Post-processing where sensitivities as well as additional information are computed.

In the preprocessing stage we seek to find characteristic values for the parameters and the loss function. These characteristic values are used to determine the temperature and regularization factor in the PDF p (2).

In the sampling stage we first determine the temperature and regularization factor. Subsequently an MCMC sampler is run to collect samples from (2).

In the post-processing stage we compute sensitivities by evaluating the gradient of the loss function at the samples drawn in the sampling stage ii. In addition, the robustness

of the sensitivities with respect to perturbations in the temperature and the parameter correlations are extracted from the existing samples and gradient evaluations. These two pieces of information are by-products of computing sensitivities and require no additional computation.

These three stages are described in Subsections 3.1, 3.2, and 3.3, respectively. The method is summarized as a whole in Subsection 3.4.

3.1 Preprocessing stage

Characteristic magnitudes for θ and \mathcal{L} are needed to determine the regularization factor and temperature. To this end we introduce two auxiliary computations as a preprocessing step.

The first auxiliary computation runs an optimization routine to minimize \mathcal{L} ; the choice of optimizer is not essential here. Let θ^* be the minimizing parameter vector. For our purposes it is acceptable if θ^* is not the global minimizer of \mathcal{L} because we only need to capture characteristic magnitudes.

The second auxiliary computation uses θ^* to determine the range of loss function values that our MCMC sampler should explore. Let $c > 0$, and let $\Theta = (\Theta_1, \Theta_2, \dots, \Theta_n)$ be a random vector defined by

$$\Theta_k \sim \mathcal{U}[(1 - c)\theta_k^*, (1 + c)\theta_k^*],$$

where all the Θ_k 's are independent of one another and \mathcal{U} denotes the uniform distribution. Hence, Θ represents uniform uncertainty of $c\%$ about θ^* .

Determining c is an application-dependent problem. In fact, its determination is the only portion of our proposed method that cannot be automated. To choose c , we suggest fixing a value for c , sampling from Θ , and visualizing the statistical model output corresponding to the sample. Varying c and replicating this visualization several times for each c allow the user to determine a choice of c that yields reasonable model outputs. This step is highly subjective and application dependent; however, it is a very natural means of inserting user specification without requiring extensive understanding of the model. Taking large values for c will result in the PDF p giving significant probability to regions of the parameter space yielding poor fits, and thus hence sensitivity indices that are not useful. Taking small values for c will result in the PDF p giving significant probability to regions of the parameter space near local minima, thus making the sensitivity indices local. Since the choice of c is not clearly defined, the robustness of the sensitivity indices with respect to perturbations in c is highly relevant; this is indirectly addressed by Theorem 2.

Once c is specified, then a threshold M , which is used to compute the regularization factor and temperature (see Subsection 3.2.1 and Subsection 3.2.2), may be easily computed via Monte Carlo integration. We define the threshold

$$M = \mathbb{E}(\mathcal{L}(\Theta)). \tag{4}$$

Note that the expectation in (4) is computed with respect to the independent uniform measure; all other expectations in the paper are computed with respect to the PDF p (2).

3.2 Sampling stage

We use an MCMC method to sample from p (2) through evaluations of the unnormalized density q (1). Then the S_k 's may be computed through evaluations of $\nabla \mathcal{L}$ at the sample points. Many MCMC methods may be used to sample p ; see, for example [25–30].

Determining which MCMC method to use and when it has converged may be challenging. Convergence diagnostics [31, 32] have been developed that may identify when the chain has not converged; however, they all have limitations and cannot ensure convergence [33]. In Section 4, adaptive MCMC [27] is used with the convergence diagnostic from [34].

Assuming that an MCMC sampler is specified, we focus on determining the temperature and regularization factors in Subsections 3.2.1 and 3.2.2, respectively.

3.2.1 Determining the regularization factor

To determine the regularization factor λ , consider the function

$$\mathcal{L}_\lambda(\theta) = \mathcal{L}(\theta) + \lambda \|\theta\|_2^2.$$

The PDF p gives greatest probability to regions where \mathcal{L}_λ is small. If $\lambda \|\theta\|_2^2$ is small relative to $\mathcal{L}(\theta)$, then the local minima of \mathcal{L}_λ are near the local minima of \mathcal{L} . Ideally we would like $\lambda = 0$, but in some cases this results in p being too heavy tailed. Instead we may require that $\lambda \|\theta\|_2^2 \approx \nu \mathcal{L}_\lambda(\theta)$ for some $\nu \in (0, 1)$; that is, the regularization term contributes ν percent of the value of \mathcal{L}_λ . Setting $\lambda \|\theta\|_2^2 = \nu \mathcal{L}_\lambda(\theta)$ and replacing $\mathcal{L}(\theta)$ and θ with M and θ^* , we get

$$\lambda = \frac{\nu M}{(1 - \nu) \|\theta^*\|_2^2}. \quad (5)$$

In practice we suggest begining with $\nu = 0$. If the MCMC sampler yields heavy-tailed distributions that converge slowly, then ν may be increased to aid the convergence. This case is illustrated in Section 4.

3.2.2 Determining the temperature

To determine the temperature δ , we first define

$$M_\lambda = M + \lambda \|\theta^*\|_2^2.$$

We seek to find δ so that $\mathcal{L}_\lambda(\theta) \leq M_\lambda$ with probability α ; $\alpha = .99$ is suggested to mitigate wasted computation in regions where θ yields a poor fit. Let $C = \{\theta \in B | \mathcal{L}_\lambda(\theta) \leq M_\lambda\}$. We note that C is a Lebesgue measurable set since \mathcal{L}_λ is continuous and B is Lebesgue measurable. We define the function $\Delta : [\delta_{\min}, \infty) \rightarrow [0, 1]$ by

$$\Delta(\delta) = \int_C p(\theta) d\theta. \quad (6)$$

Then $\Delta(\delta)$ gives the probability that $\mathcal{L}_\lambda(\theta) \leq M_\lambda$. The optimal temperature δ is the solution of $\Delta(\delta) = \alpha$. Four results are given below showing that Δ possesses advantageous properties making the nonlinear equation $\Delta(\delta) = \alpha$ easily solvable. The proofs are given in the appendix.

Proposition 1. *If $\int_B \mathcal{L}_\lambda(\theta) e^{-\delta_{\min} \mathcal{L}_\lambda(\theta)} d\theta < \infty$, then Δ is differentiable on (δ_{\min}, ∞) with*

$$\Delta'(\delta) = (-1 + \Delta(\delta)) \int_C \mathcal{L}_\lambda(\theta) p(\theta) d\theta + \Delta(\delta) \int_{B \setminus C} \mathcal{L}_\lambda(\theta) p(\theta) d\theta. \quad (7)$$

Proposition 2. *If $\int_B \mathcal{L}_\lambda(\theta) e^{-\delta_{\min} \mathcal{L}_\lambda(\theta)} d\theta < \infty$, then Δ is a strictly increasing function on (δ_{\min}, ∞) .*

Propositions 1 and 2 yield desirable properties of Δ . The assumption that $\mathcal{L}_\lambda(\theta) e^{-\delta_{\min} \mathcal{L}_\lambda(\theta)}$ is integrable is necessary for $\Delta'(\theta)$ to be well defined. Note that this assumption follows from Assumption I when B is bounded. Theorem 1 and Corollary 1 below give existence and uniqueness, respectively, for the solution of $\Delta(\delta) = \alpha$ under mild assumptions.

Theorem 1. *If B is a bounded set and $\exists \theta' \in B$ such that $\mathcal{L}_\lambda(\theta') < M_\lambda$, then $\forall \alpha \in (0, 1)$ $\exists \delta > \delta_{\min}$ such that $\Delta(\delta) > \alpha$.*

Corollary 1. *If $\alpha \in (\Delta(\delta_{\min}), 1)$, B is a bounded set, and $\exists \theta' \in B$ such that $\mathcal{L}_\lambda(\theta') < M_\lambda$, then $\Delta(\delta) = \alpha$ admits a unique solution.*

The assumption that B is bounded is reasonable in most applications; A may be unbounded, but B is restricted to relevant solutions that will typically be bounded. The assumption that $\mathcal{L}_\lambda(\theta') < M_\lambda$ means that M_λ is not chosen as the global minimum, which should always hold in practice. The assumption that $\alpha \in (\Delta(\delta_{\min}), 1)$ is necessary for existence. Typically $\Delta(\delta_{\min})$ is much less than 1, while α is chosen close to 1, so this assumption also holds in most cases.

In summary, under mild assumptions $\Delta(\delta) = \alpha$ is a scalar nonlinear equation admitting a unique solution and Δ possesses nice properties (monotonicity and differentiability). Further, $\Delta(\delta)$ and $\Delta'(\delta)$ may be approximated simultaneously by running MCMC. The challenge is that evaluating $\Delta(\delta)$ and $\Delta'(\delta)$ in high precision requires running a long MCMC chain. In fact, $\Delta'(\delta)$ is significantly more challenging to evaluate than $\Delta(\delta)$. For this reason we suggest using derivative-free nonlinear solvers which will still be efficient since Δ is a well-behaved function. In the spirit of inexact Newton methods [35], shorter chains may be run for the early iterations solving $\Delta(\delta) = \alpha$ and the precision increased near the solution. In practice, relatively few evaluations of Δ are needed because of its properties, shown above.

3.3 Post-processing stage

Having attained samples from p (2), the sensitivities (3) may be estimated by evaluating ∇L at the sample points and forming the Monte Carlo estimator for the expectations in (3). In addition to computing these sensitivities, we may extract two other useful pieces of information, namely, the robustness of the sensitivities with respect to perturbations in the temperature and the parameter correlations. These are described in Subsections 3.3.1 and 3.3.2, respectively.

3.3.1 Robustness with respect to the temperature

As a result of the uncertainty in the determination of δ (choice of c , computation of M , solution of $\Delta(\delta) = \alpha$), we analyze the robustness of the sensitivities with respect to δ . Consider the functions

$$F_k : (\delta_{\min}, \infty) \rightarrow \mathbb{R},$$

$$\delta \mapsto \left(\int_B |\theta_k| \left(\frac{e^{-\delta \mathcal{L}_\lambda(\theta)}}{\int_B e^{-\delta \mathcal{L}_\lambda(\tilde{\theta})} d\tilde{\theta}} \right) d\theta \right) \left(\int_B \left| \frac{\partial \mathcal{L}}{\partial \theta_k}(\theta) \right| \left(\frac{e^{-\delta \mathcal{L}_\lambda(\theta)}}{\int_B e^{-\delta \mathcal{L}_\lambda(\tilde{\theta})} d\tilde{\theta}} \right) d\theta \right)$$

$k = 1, 2, \dots, n$; clearly $F_k(\delta) = S_k$. Theorem 2 gives the derivative of the sensitivity index with respect to the temperature δ , namely, $F'_k(\delta)$.

Theorem 2. *If $\int_B \mathcal{L}_\lambda(\theta) e^{-\delta_{\min} \mathcal{L}_\lambda(\theta)} d\theta$, $\int_B \mathcal{L}_\lambda(\theta) |\theta_k| e^{-\delta_{\min} \mathcal{L}_\lambda(\theta)} d\theta$, and $\int_B \mathcal{L}_\lambda(\theta) \left| \frac{\partial \mathcal{L}}{\partial \theta_k}(\theta) \right| e^{-\delta_{\min} \mathcal{L}_\lambda(\theta)} d\theta$ exist and are finite, then F_k is differentiable with*

$$F'_k(\delta) = -\text{Cov}(|\theta_k|, \mathcal{L}_\lambda(\theta)) \mathbb{E} \left(\left| \frac{\partial \mathcal{L}}{\partial \theta_k}(\theta) \right| \right) - \mathbb{E}(|\theta_k|) \text{Cov} \left(\left| \frac{\partial \mathcal{L}}{\partial \theta_k}(\theta) \right|, \mathcal{L}_\lambda(\theta) \right), \quad (8)$$

where $\text{Cov}(\cdot, \cdot)$ is the covariance operator.

Theorem 2 allows $F'_k(\delta)$ to be computed from the samples and function evaluations used to compute S_k . For small h , $F_k(\delta + \delta h) \approx F_k(\delta) + h \delta F'_k(\delta)$ so the robustness of S_k may be estimated without any further computational expense.

Since the magnitude of S_k may depend on δ , it is useful to normalize for each h when assessing robustness. We define

$$\hat{F}_k(\delta + \delta h) = \frac{F_k(\delta) + h \delta F'_k(\delta)}{\sum_{j=1}^n (F_j(\delta) + h \delta F'_j(\delta))}, \quad k = 1, 2, \dots, p, \quad (9)$$

which may be plotted for $h \in (-h_{\max}, h_{\max})$ to assess robustness. Since this is only a local estimate we suggest taking $h_{\max} = \frac{1}{10}$, reflecting a 10% uncertainty about δ .

3.3.2 Extracting parameter correlations

Parameters are typically correlated, and the correlation information is a valuable complement to the sensitivity indices. For instance, if \mathcal{G} is sensitive to two parameters that are highly correlated, then it may be possible to remove one of them from \mathcal{G} since the other may compensate. In addition, the correlations may reveal parameter mis-specifications in \mathcal{G} .

The strength and nature of the correlations in θ are typically not known a priori. Correlation coefficients may be computed from the MCMC samples and returned as a by-product of computing sensitivity indices. The Pearson correlation coefficient (PCC) is commonly used to measure correlations from sampled data. Other measures of correlation may be interchanged within our framework as well.

3.4 Summary of the method

This subsection summarizes our proposed method. The method is divided into three algorithms, one for each stage described in Section 3.

Algorithm 1 performs the auxiliary computations of Subsection 3.1. Note that determining c in line 2 is the only application-specific portion of the proposed method; user discernment is necessary to choose c .

Algorithm 2 requires the user to specify the parameter ν from Subsection 3.2.1, the parameter α from Subsection 3.2.2, and the number of MCMC samples N . We suggest starting with $\nu = 0$ and rerunning Algorithm 2 with a larger ν if the convergence results indicate that the PDF is heavy tailed. The choice of N may be difficult; however, more samples may be appended after an initial run so N can be adapted without any wasted computation.

Algorithm 3 is a simple post-processing of the MCMC samples to compute sensitivity indices, robustness estimates, and parameter correlations. One may also perform convergence diagnostics on the MCMC estimators of $\mathbb{E} \left(\left| \frac{\partial \mathcal{L}}{\partial \theta_k}(\theta) \right| \right)$, $k = 1, 2, \dots, n$, along with Algorithm 3.

Algorithm 1 Auxiliary Computation

- 1: compute $\theta^* = \arg \min \mathcal{L}(\theta)$ via some optimization routine
- 2: determine c through visualization of model outputs
- 3: estimate M via Monte Carlo integration

Algorithm 2 Sampling

- 1: **function** (ν, N, α)
- 2: compute λ using (5)
- 3: solve $\Delta(\delta) = \alpha$
- 4: run MCMC sampler to draw N samples from p (2)
- 5: store MCMC samples in a matrix X
- 6: test convergence of the sampler
- 7: **end function**

Algorithm 3 Sensitivities, Perturbations, and Correlations

- 1: evaluate $\nabla \mathcal{L}$ at points in X
- 2: estimate S_k , $k = 1, 2, \dots, n$
- 3: estimate $F'_k(\delta)$, $k = 1, 2, \dots, n$
- 4: compute empirical correlation matrices from X

4 Numerical results

In this section we apply the proposed method to two problems. The first is a synthetic test problem meant to illustrate the methodological details described in Section 3. The

second is our motivating application where \mathcal{G} is a space-time hierarchical Gaussian process used for wind speed forecast [11].

4.1 Synthetic test problem

This synthetic problem validates the proposed method of GSA and illustrate its properties on a simple example. We demonstrate the difficulty of MCMC sampling with heavy tailed distributions and how the regularization factor (5) alleviates this problem.

Consider a space-time process governed by the function

$$f(x, t) = S(x)T(t), \quad (10)$$

where

$$S(x) = \alpha_0 + \alpha_1 x + \alpha_2 x^2, \text{ and}$$

$$T(t) = \beta_0 + \beta_1 e^{-\gamma t} \cos\left(\frac{2\pi}{100}t\right) + \beta_2 \sin\left(\frac{2\pi}{100}t\right) + \beta_3 \frac{1}{1 + e^{-1(t-50)}}$$

with $x \in [0, 1]$, $t \in [0, 100]$, and

$$\begin{aligned} \theta &= (\beta_0, \beta_1, \beta_2, \beta_3, \gamma, \alpha_0, \alpha_1, \alpha_2) \\ &= (2, 10, 3, .01, .01, 1, .01, 1). \end{aligned} \quad (11)$$

We draw 15^2 samples from (10) on a uniform grid of $[0, 1] \times [0, 100]$, which gives data

$$\{(x_i, t_i, f(x_i, t_i))\}_{i=1}^{225}.$$

A statistical model \hat{f} parameterized in the same form as (10) is proposed, but the parameters are assumed to be unknown. They are determined by minimizing the model misfit loss function

$$\mathcal{L}(\theta) = \frac{1}{225} \sum_{i=1}^{225} (f(x_i, t_i) - \hat{f}(x_i, t_i))^2.$$

Analytic solutions for the sensitivities are intractable; however, we can validate our results by comparing them with our knowledge of the true model that generated the data. In particular, the relative importance of the parameters is clear by examining (10) and (11). We expect β_1 to be the most important parameter and β_3 and α_1 to be the least important parameters.

The proposed method is used with $N = 10^5$, $\alpha = .99$, $c = .1$, and $h_{max} = .1$. Five independent chains are generated from overdispersed initial iterates using adaptive MCMC [27]. When $\nu = \lambda = 0$, the MCMC sampler fails to converge because the tail of p is too heavy. To illustrate this, Figure 1 shows the iteration history for the parameter β_1 in each of the five chains after a burn-in period is discarded. The two leftmost frames indicate that p is heavy tailed; the other three chains never reach the tail. A heavy-tailed

PDF such as this requires extensive sampling, which makes the reliable computation of sensitivity indices intractable. Therefore, we use regularization to alleviate this problem by increasing ν as we monitor the sampler's convergence. We find that $\nu = .2$ yields converged chains with $N = 10^5$ samples. The chains are deemed convergent by using the potential scale reduction factor (PSRF) [34] as well as visualizing the iteration histories and histograms from each of the five chains.

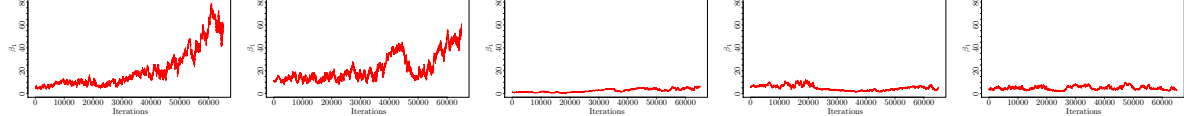


Figure 1: Iteration history for parameter β_1 . Each frame corresponds to an independent chain.

Plotting the iteration history of \mathcal{L}_λ indicates that a burn-in of 3.5×10^4 is sufficient. Then the remaining samples from the five chains are pooled together so that sensitivities and correlations may be computed from them. Figure 2 shows the sensitivity indices and Pearson correlation matrix computed from the pooled samples. These results are consistent with our expectations, β_1 is seen as the most important parameter and α_1 as the least important. Two primarily blocks are seen in the correlation plot representing the set of spatial variables and the set of temporal variables. Negative correlations are observed on the off diagonal blocks since the spatial and temporal variables are multiplied by one another and hence are inversely related.

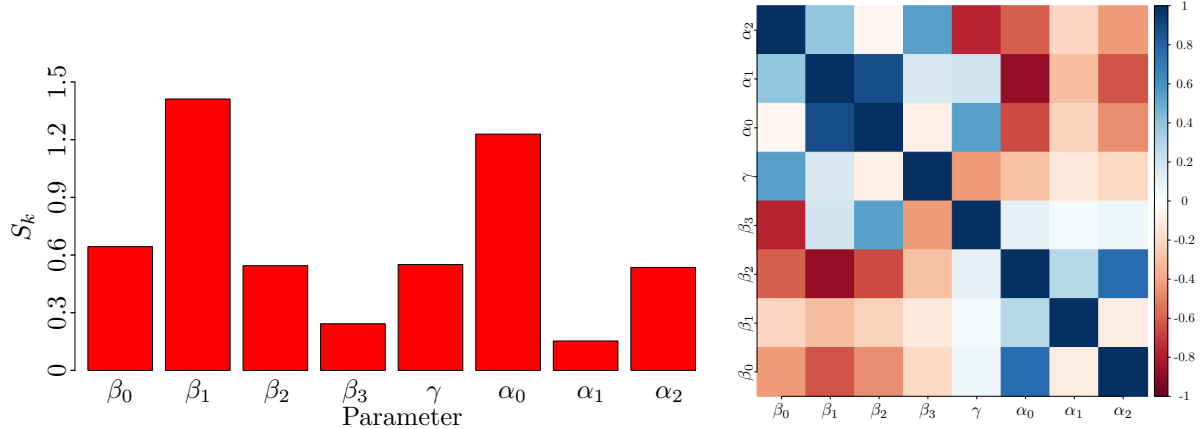


Figure 2: Sensitivity indices (left) and Pearson correlation coefficients of the parameters (right) for the synthetic test problem.

Figure 3 displays (9) plotted for $h \in (-\frac{1}{10}, \frac{1}{10})$, $k = 1, 2, \dots, 8$. The horizontal lines indicate that errors in determining δ are immaterial since the analysis would be unchanged by perturbing δ .

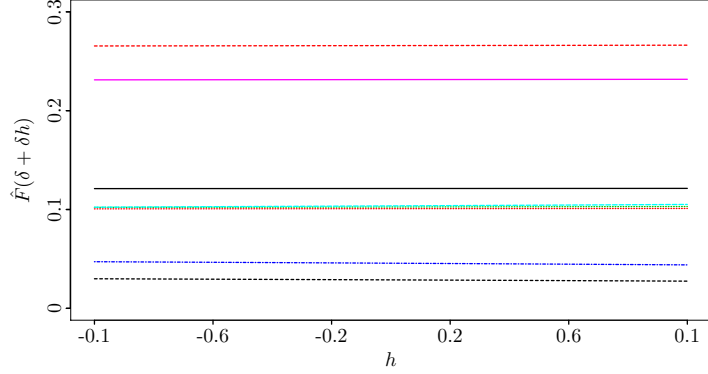


Figure 3: Sensitivity index perturbations for the synthetic test problem. Each line corresponds to a given parameter.

4.2 Analysis of a space-time Gaussian process

In this section we apply the proposed method to analyze the motivating statistical model [11]. The model aims at forecasting wind speed by fusing two heterogeneous datasets: numerical weather prediction model (NWP) outputs and physical observations. Let Y_{NWP} denote the output of the NWP model and Y_{Obs} denote the observed measurements. They are modeled as a bivariate space-time Gaussian process specified in terms of mean and covariance structures as follows,

$$\begin{pmatrix} Y_{\text{Obs}} \\ Y_{\text{NWP}} \end{pmatrix} \sim \mathcal{N} \left(\begin{pmatrix} \mu_{\text{Obs}}(\theta) \\ \mu_{\text{NWP}}(\theta) \end{pmatrix}, \begin{pmatrix} \Sigma_{\text{Obs}}(\theta) & \Sigma_{\text{Obs}, \text{NWP}}(\theta) \\ \Sigma_{\text{Obs}, \text{NWP}}^T(\theta) & \Sigma_{\text{NWP}}(\theta) \end{pmatrix} \right), \quad (12)$$

where θ is the set of parameters that describe the shapes of the means and covariances. The model is expressed in a hierarchical conditional manner to avoid the specification of the full joint covariance in (12), indeed the mean and covariance of the distributions $(Y_{\text{Obs}}|Y_{\text{NWP}}) \sim \mathcal{N}(\mu_{\text{Obs}|NWP}, \Sigma_{\text{Obs}|NWP})$ and $Y_{\text{NWP}} \sim \mathcal{N}(\mu_{\text{NWP}}, \Sigma_{\text{NWP}})$ are specified in time, geographical coordinates, and parameters from the numerical model (the land-use parameter). More precisely,

$$\mu_{\text{NWP}}(t, s) = (\alpha_0 \text{LU}(s) + \alpha_1 \text{Lat}(s) + \alpha_2 \text{Long}(s)) f(t), \quad (13)$$

where s is a spatial location, t is time, $f(t)$ represents a sum of temporal harmonics with daily, half-daily and 8hr-periodicities, $\text{LU}(s)$ is a categorical variable that represents the land-use associated with location s , Lat and Long are the latitude and longitude coordinates.

$$\Sigma_{\text{NWP}}(., s_i; ., s_j) = \text{Cov}(Y_{\text{NWP}}(., s_i), Y_{\text{NWP}}(., s_j)) = (\Psi(s_i) \Gamma_0 \Psi(s_j)^T) + \delta_{i-j} \Gamma_{\text{LU}(s_i)}, \quad (14)$$

$\Gamma_0, (\Gamma_{\text{LU}(s_i)})_{i=1..I}$ are temporal squared exponential covariances expressed as

$$\Gamma_{\cdot}(t_k, t_l) = \sigma_{\cdot} \exp(-\rho_{\cdot}(|t_k - t_l|)^2) + \delta_{k-l} \gamma_{\cdot},$$

where δ_{k-l} is the Kronecker delta, σ , ρ , and γ are parameters to be estimated. $(\Gamma_{\text{LU}(s_i)})_{i=1..I}$ are land-use specific terms, and Ψ is linear in the latitude and longitude coordinates

and quadratic in time. The parameters $\alpha_0, \alpha_1, \alpha_2$, along with the parameters of $f(t)$, $(\Gamma_{s_i})_{i=0..I}$ and Ψ , will be estimated during the maximum likelihood procedure. We will denote the collection of all these parameters by θ_{NWP} .

The conditional distribution is expressed through its mean and covariance:

$$\mu_{Obs|NWP}(t, s) = \mu(t, s) + (\Lambda Y_{NWP})(t, s), \quad (15)$$

where $\mu(t, s)$ is written similarly to $\mu_{NWP}(t, s)$ as a product of temporal harmonics and a linear combination of the coordinates latitude and longitude. Λ is a projection matrix specified in time, latitude, longitude and the land-use parameter. The covariance $\Sigma_{Obs|NWP}$ is parametrized with a similar shape to (14) with a different set of parameters. Parameters of these functions are denoted as $\theta_{Obs|NWP}$ in the following and will be estimated by maximum likelihood.

This model is fitted by maximum likelihood on the two datasets with respect to the parameters $\theta = (\theta_{NWP}, \theta_{Obs|NWP})$. The negative log likelihood of the model can be decomposed as

$$\mathcal{L}(\theta) = \mathcal{L}_{NWP}(\theta_{NWP}) + \mathcal{L}_{Obs|NWP}(\theta_{Obs|NWP}), \quad (16)$$

where $\mathcal{L}_{NWP}(\theta_{NWP})$ and $\mathcal{L}_{Obs|NWP}(\theta_{Obs|NWP})$ are the negative log likelihoods for the marginal distribution of Y_{NWP} and the conditional distribution $Y_{Obs|NWP}$, respectively. Since the model decomposes in this way, we will consider analysis of the parameters in Y_{NWP} and $Y_{Obs|NWP}$ separately. Our dataset consists of 27 days of measurements from August 2012; details may be found in [11]. The parameter sensitivity during the first 13 days for Y_{NWP} and $Y_{Obs|NWP}$ is analyzed in Subsection 4.2.1 and Subsection 4.2.2, respectively. Inferences are drawn from this analysis and validated using the later 14 days of data in Subsection 4.2.3.

4.2.1 Parameter sensitivity analysis for Y_{NWP}

In this subsection we apply the proposed method to determine the sensitivity of the marginal model for Y_{NWP} to its 41 parameters during a 13-day period. The sensitivities being computed are with respect to the parameters in θ_{NWP} , but for notational simplicity we will denote them by θ in this subsection.

In order to determine θ^* (line 1 of Algorithm 1), the L-BFGS-B algorithm is used to minimize \mathcal{L}_{NWP} . Visualizing the model predictions for various choices of c yields $c = .35$ (line 2 of Algorithm 1). Then M (4) is estimated with $\ell = 5000$ Monte Carlo samples (line 3 of Algorithm 1). It returns an estimate $M = 4160$ with standard deviation 2; hence ℓ is considered to be sufficiently large. These steps complete the preprocessing stage by providing characteristic values for the parameters θ and the loss function \mathcal{L} .

The PDF p is found to be heavy tailed, so $\nu = .1$ is chosen to reduce this effect. Then the equation $\Delta(\delta) = \alpha$ is solved with $\alpha = .99$ by evaluating Δ and manually updating δ . The solution $\delta = .07$ is obtained. This converged in very few iterations because of the nice properties of the equation $\Delta(\delta) = \alpha$. Any other derivative-free nonlinear solver may be used in our framework; however, manual tuning is preferable in many cases because of

the simplicity of the equation and the stochasticity of the function evaluations. Having determined ν and δ , the PDF p from which we draw samples is now well defined.

Adaptive MCMC [27] is used with a desired acceptance rate of .15. Five chains of length $N = 4 \times 10^5$ each are generated independently from overdispersed initial iterates, and the first 10^5 iterates are discarded as burn-in. The PSRF convergence diagnostic from [34] is used on θ_k and $\frac{\partial \mathcal{L}}{\partial \theta_k}$ separately to assess the convergence of each. The PSRFs for all parameters lie in the intervals $(1, 1.025)$ and $(1, 1.048)$, respectively. Other visual diagnostics are applied as well, along with comparing sensitivity indices from each of the chains. The sensitivity estimation appears to converge.

Figure 4 displays the sensitivity indices estimated from each of the chains. The five different colors represent the five different chains; their comparability demonstrates that MCMC estimation errors are negligible. The intercept terms in the mean and the covariance kernel parameters are the most influential. The terms parameterizing Ψ are less influential, particularly the quadratic temporal terms.

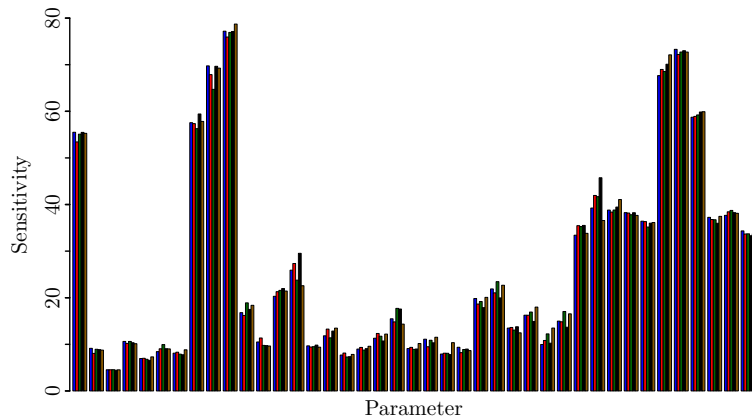


Figure 4: Sensitivity indices for Y_{NWP} . The five colors represent the sensitivity indices computed from each of the five chains.

As discussed in Subsection 3.3.1, the robustness of the sensitivities with respect to errors in δ may be estimated as a by-product of computing sensitivities. Figure 5 displays (9) plotted for $h \in (-1/10, 1/10)$, $k = 1, 2, \dots, 41$. Most of the curves are nearly horizontal, and those that are not horizontal display small variation that does not change the resulting inference. Thus the sensitivities are robust with respect to δ , and hence any errors made when determining δ are negligible.

As mentioned in Subsection 3.3.2, parameter correlation information is a useful complement to sensitivity indices. Figure 6 displays the empirical Pearson correlation matrix computed from the 1.5×10^6 MCMC samples retained after removing burn-in and pooling the chains. Strong positive correlations are observed between the three land-use dependent spatial intercepts in the mean. Strong negative correlations are observed between the temporal range ρ and the nugget term γ parameterizing the land-use specific covariance kernels $\Gamma_{LU(s_i)}$. This correlation is expected since the nugget term represents the variance of the signal that is not explained by the exponential part.

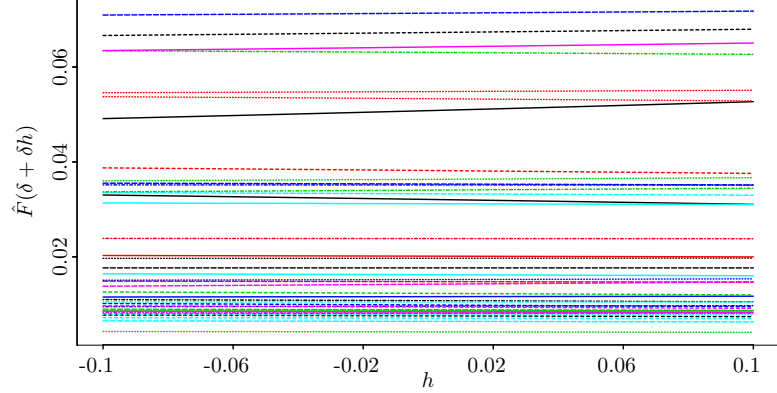


Figure 5: Sensitivity index perturbations for Y_{NWP} . Each line corresponds to a given parameter.

4.2.2 Parameter sensitivity analysis for $Y_{\text{Obs}}|Y_{\text{NWP}}$

In this subsection we apply the proposed method to determine the sensitivity of the model for $Y_{\text{Obs}}|Y_{\text{NWP}}$ to its 54 parameters during the same 13-day period used in Subsection 4.2.1. The sensitivities being computed are with respect to the parameters in $\theta_{\text{Obs}|NWP}$, but for notational simplicity we will denote them by θ in this subsection.

In a similar fashion to Subsection 4.2.1, the L-BFGS-B algorithm is used to determine θ^* (line 1 of Algorithm 1). Visualizing the model predictions for various choices of c yields $c = .05$ (line 2 of Algorithm 1). Then M (4) is estimated with $\ell = 5000$ Monte Carlo samples (line 3 of Algorithm 1). It returns an estimate $M = 2973$ with standard deviation 2; hence ℓ is considered to be sufficiently large. These steps complete the preprocessing stage by providing characteristic values for the parameters θ and the loss function \mathcal{L} . One may note that c and M are significantly smaller for $Y_{\text{Obs}}|Y_{\text{NWP}}$ than for Y_{NWP} . Their difference is unsurprising since Y_{NWP} and $Y_{\text{Obs}}|Y_{\text{NWP}}$ model two different processes.

The PDF p is found to be heavy tailed, so $\nu = .15$ is chosen to reduce the tail of p . Analogously to Subsection 4.2.1, $\Delta(\delta) = \alpha = .99$ is solved yielding $\delta = .06$ (line 3 of Algorithm 2).

Adaptive MCMC [27] is used with a desired acceptance rate of $.15$. Five chains of length $N = 4 \times 10^5$ each are generated independently from overdispersed initial iterates, and the first 10^5 iterates are discarded as burn-in. The convergence diagnostic from [34] is used on θ_k and $\frac{\partial \mathcal{L}}{\partial \theta_k}$ separately to assess the convergence of each. The PSRFs for all parameters lie in the intervals $(1, 1.191)$ and $(1, 1.036)$, respectively. Other visual diagnostics are applied as well, along with comparing sensitivity indices from each of the chains. A few sensitivity indices have not fully converged; however, the remaining uncertainty in their estimation is sufficiently small for our purposes. These uncertain sensitivities are among the largest in magnitude. Since our goal is encouraging model parsimony, then precisely ordering the most influential parameters is of secondary importance.

Figure 7 displays the sensitivity indices estimated from each of the chains. The five different colors represent the five different chains. The sensitivities with greatest uncertainties are demonstrated by the differences in their estimated values in each chain;

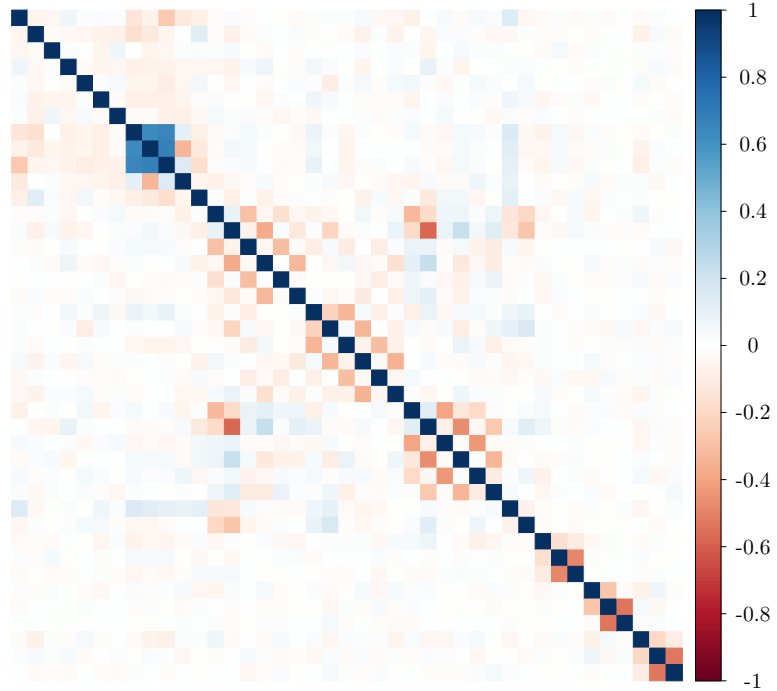


Figure 6: Pearson correlation coefficients for the parameters of Y_{NWP} .

however, these discrepancies are sufficiently small that they do not alter our resulting inference. The longitudinal terms in the mean and Ψ are observed to have little influence since their sensitivity indices are nearly zero. The most influential parameters are the spatial weights in the matrix Λ which acts on Y_{NWP} .

As discussed in Subsection 3.3.1, the robustness of the sensitivities with respect to errors in δ may be estimated as a by-product of computing sensitivities. Figure 8 displays (9) plotted for $h \in (-\delta/10, \delta/10)$, $k = 1, 2, \dots, 54$. Most of the curves are nearly horizontal, and those that are not horizontal display small variation that does not change the resulting inference.

As mentioned in Subsection 3.3.2, parameter correlation information is a useful complement to sensitivity indices. Figure 9 displays the empirical Pearson correlation matrix computed from the 1.5×10^6 MCMC samples retained after burn-in and pooling the chains. Strong correlations are observed between the spatial weights in the matrix Λ . Similar to Y_{NWP} , strong negative correlations are also observed between the temporal range ρ and the nugget term γ of the land-use specific covariance kernels.

4.2.3 Inference and validation of results

In some cases with mathematical models one may set a threshold and fix or remove all parameters whose sensitivity is below the threshold. This approach is not suitable for statistical models because the parameters must be understood in light of their contribution

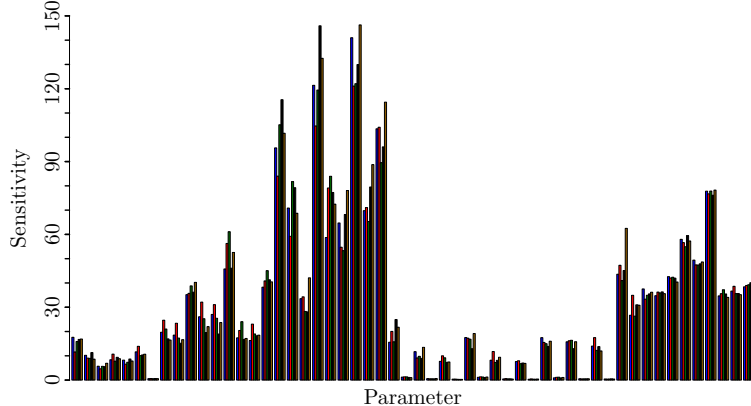


Figure 7: Sensitivity indices for $Y_{\text{Obs}}|Y_{\text{NWP}}$. The five colors represent the sensitivity indices computed from each of the five chains.

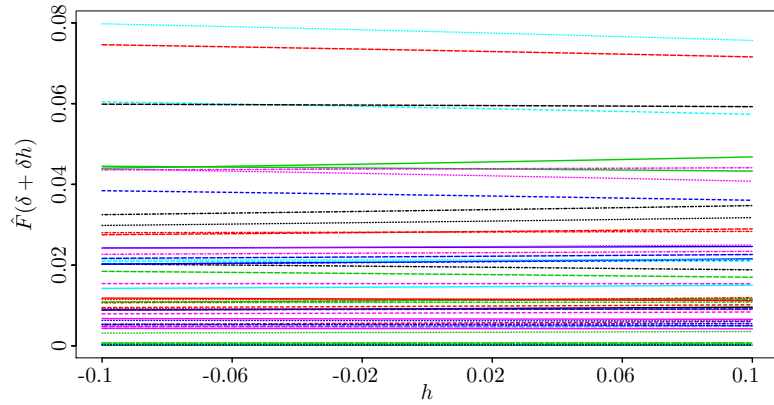


Figure 8: Sensitivity index perturbations for $Y_{\text{Obs}}|Y_{\text{NWP}}$. Each line corresponds to a given parameter.

to the model structure and their correlation with other parameters. Using the results of Subsection 4.2.1, and considerations of the model structure, we determine that the Y_{NWP} model is insensitive to the temporal quadratic terms in the parameterization of Ψ . Similarly, coupling the results of Subsection 4.2.2, and the model structure, we determine that the $Y_{\text{Obs}}|Y_{\text{NWP}}$ model is insensitive to several of the longitude terms. Specifically, the longitude term in the parameterization of the mean and the nine longitude terms in the parameterization of Ψ . This conclusion confirms what one would expect from the physics considerations. The flow is predominantly east-west and thus the north-south correlation is relatively weaker. The east-west information is likely to be well captured by Y_{NWP} and hence is not needed in $Y_{\text{Obs}}|Y_{\text{NWP}}$.

The 16 insensitive parameters are removed from the model, yielding a more parsimonious model that we refer to as the reduced model. To validate our inferences, we use the original model and the reduced model for prediction on the other 14 days of data we have available but did not use in the sensitivity analysis. Leave-one-out cross-validation is used to fit each of the models and assess their predictive capabilities.

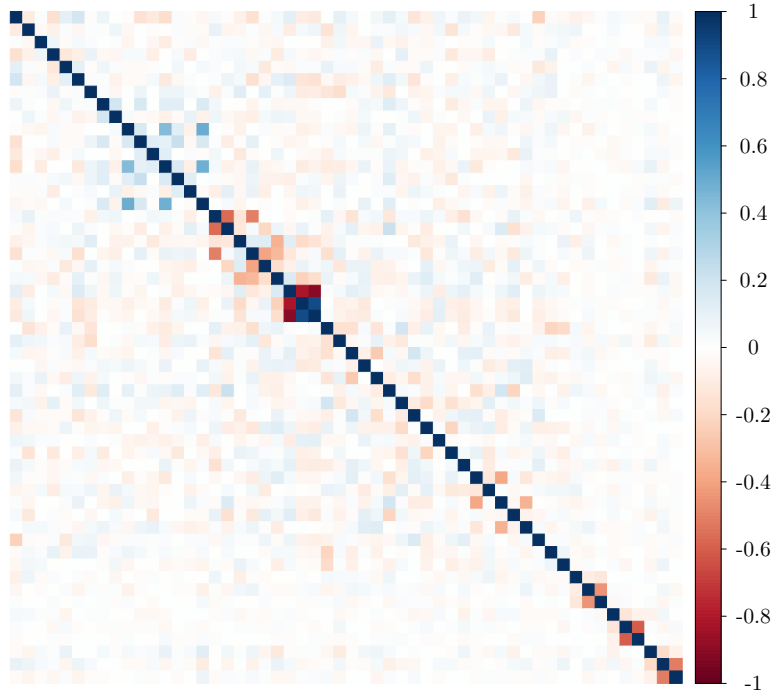


Figure 9: Pearson correlation coefficients for the parameters of $Y_{\text{Obs}}|Y_{\text{NWP}}$.

We simulated 1,000 scenarios for each of the 14 days and use two metrics to quantify the predictive capacity of the full and reduced models, namely, the energy score and the root mean square error. The energy score [36, 37] is computed for the joint distribution of all spatial locations at each day; hence, 14 energy scores are computed. The root mean square error is computed as the square root of the time average squared error at each spatial location; hence, there are 11 root mean square errors. Figure 10 displays the energy scores on the left and root mean square errors on the right. The reduced model has slightly smaller (and hence better) energy scores and root mean square errors in the majority of the cases. The sum of energy scores for full model and reduced model is 121.1 and 120.7, respectively. The sum of root mean squared errors for the full model and reduced model is 11.4 and 11.3, respectively.

To further illustrate the difference between the full and reduced models, we display the simulated scenarios for a typical case. Specifically, we take the spatial location with median root mean square error and six days with median energy score and plot the 1,000 scenarios along with the observed data. Figure 11 displays the results with the full model on the left and reduced model on the right.

We have thus simplified the parameterization of the model from having 95 parameters to 79. The reduced model has equal or better predictive capability and is simpler to fit and analyze. Further, the reduced model typically has fewer outlying scenarios, as evidenced in Figure 11.

For this application we observed a strong insensitivity of $Y_{\text{Obs}}|Y_{\text{NWP}}$ to some of its

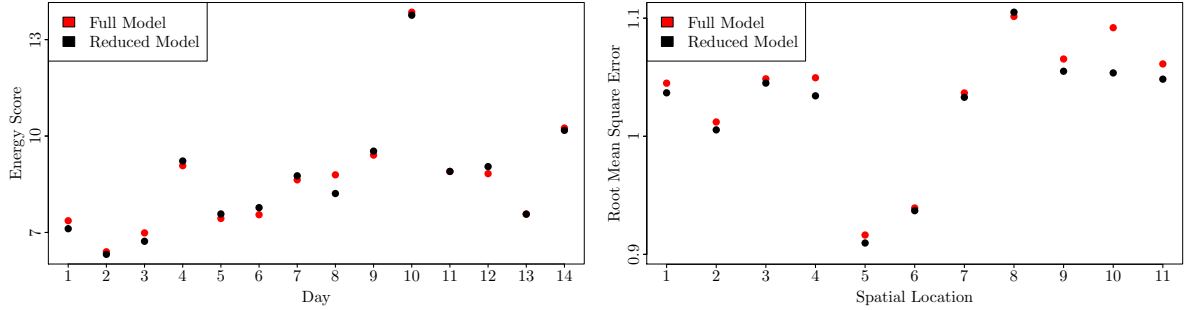


Figure 10: Left: energy scores for each of the 14 days being predicted; right: root mean square error for each of the 11 spatial locations being predicted. The full model is red and the reduced model is black.

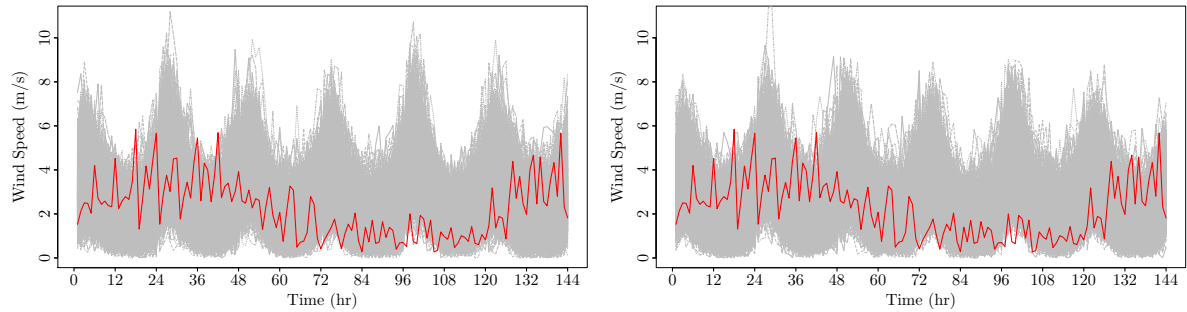


Figure 11: Predictions using the full model (left) and reduced model (right) for 6 days at a fixed spatial location. The red curve is the observed wind speed and the grey curves are 1000 simulations generated from each model.

terms contributing longitudinal information. This is likely because the Y_{NWP} model captures longitudinal information well and hence the Gaussian process does not need to fit terms contributing longitudinal information. Thus, inferences may also be made on the data being input to the statistical model through the parameter sensitivities.

5 Conclusion

A new method for global sensitivity analysis of statistical model parameters was introduced. It addresses the challenges and exploits the problem structure specific to parameterized statistical models. The method is nearly fully automated; one step depends on the user's discretion, but this level of user specification is likely necessary for any alternative method. The proposed method also admits perturbation analysis at no additional computational cost, thus yielding sensitivities accompanied with certificates of confidence in them.

The method was motivated by, and applied to, a Gaussian process model aimed at wind simulation. Sensitivities were computed and the model parameterization simplified by removing 17% of the model parameters. This simpler model was validated and shown to provide equal or superior predictive capability compared with the original model.

Our proposed method has two primary limitations. First, it relies heavily on Markov Chain Monte Carlo sampling for which convergence diagnostics are notoriously challenging. Second, regularization may be needed to eliminate heavy-tailed distributions. Determining the regularization constant is simple in principle but may require drawing many samples to resolve. However, these limitations are classical and have been observed in various applications previously.

Global sensitivity analysis has seen much success analyzing parameter uncertainty for mathematical models. The framework presented in this paper provides the necessary tools to extend global sensitivity analysis to parameters of complex statistical models.

Acknowledgements

This material was based upon work partially supported by the National Science Foundation under Grant DMS-1127914 to the Statistical and Applied Mathematical Sciences Institute. Any opinions, findings, and conclusions or recommendations expressed in this material are those of the authors and do not necessarily reflect the views of the National Science Foundation. This material is also partially based upon work supported by the U.S. Department of Energy, Office of Science, Advanced Scientific Computing Research Program under contract DE-AC02-06CH11357 (FWP #57820).

Appendix

This appendix contains the proofs for Proposition 1, Proposition 2, Theorem 1, Corollary 1, and Theorem 2.

Proof of Proposition 1

Let $U(\delta) = e^{-\delta(\mathcal{L}_\lambda(\theta) - L_{\min})}$ and $V(\delta) = \int_B e^{-\delta(\mathcal{L}_\lambda(\theta) - L_{\min})} d\theta$. Then

$$\Delta(\delta) = \frac{1}{V(\delta)} \int_C U(\delta) d\theta.$$

By using Theorem 6.28 in [38] with $(\mathcal{L}_\lambda(\theta) - L_{\min})e^{-\delta_{\min}(\mathcal{L}_\lambda(\theta) - L_{\min})}$ dominating $U'(\delta)$, we have that $\int_C U(\delta) d\theta$ and V are differentiable with

$$\begin{aligned} \frac{d}{d\delta} \int_C U(\delta) d\theta &= - \int_C (\mathcal{L}_\lambda(\theta) - L_{\min}) U(\delta) d\theta, \\ V'(\delta) &= - \int_B (\mathcal{L}_\lambda(\theta) - L_{\min}) e^{-\delta(\mathcal{L}_\lambda(\theta) - L_{\min})} d\theta. \end{aligned}$$

Δ is differentiable since $V(\delta) > 0$, $\forall \delta > \delta_{\min}$, and applying the quotient rule for derivatives gives

$$\Delta'(\delta) = \frac{\frac{d}{d\delta} \int_C U(\delta) d\theta}{V(\delta)} - \frac{V'(\delta)}{V(\delta)} \frac{\int_C U(\delta) d\theta}{V(\delta)}.$$

Simple manipulations yields

$$\Delta'(\delta) = (-1 + \Delta(\delta)) \int_C (\mathcal{L}_\lambda(\theta) - L_{\min}) \frac{U(\delta)}{V(\delta)} d\theta + \Delta(\delta) \int_{B \setminus C} (\mathcal{L}_\lambda(\theta) - L_{\min}) \frac{U(\delta)}{V(\delta)} d\theta.$$

Writing $\frac{U(\delta)}{V(\delta)} = p(\theta)$ and using the linearity of the integral completes the proof. \square

Proof of Proposition 2

From the proof of Proposition 1 we have

$$\Delta'(\delta) = (-1 + \Delta(\delta)) \int_C (\mathcal{L}_\lambda(\theta) - L_{\min}) \frac{U(\delta)}{V(\delta)} d\theta + \Delta(\delta) \int_{B \setminus C} (\mathcal{L}_\lambda(\theta) - L_{\min}) \frac{U(\delta)}{V(\delta)} d\theta.$$

Since

$$\begin{aligned} \theta \in C &\implies \mathcal{L}_\lambda(\theta) \leq M_\lambda, \\ \theta \in B \setminus C &\implies \mathcal{L}_\lambda(\theta) > M_\lambda, \\ \Delta(\delta) &\in [0, 1], \\ \int_{B \setminus C} p(\theta) d\theta &= 1 - \Delta(\delta), \end{aligned}$$

we have

$$\begin{aligned} \Delta'(\delta) &> (-1 + \Delta(\delta)) \int_C (M_\lambda - L_{\min}) \frac{U(\delta)}{V(\delta)} d\theta + \Delta(\delta) \int_{B \setminus C} (M_\lambda - L_{\min}) \frac{U(\delta)}{V(\delta)} d\theta \\ &= (-1 + \Delta(\delta))(M_\lambda - L_{\min})\Delta(\delta) + \Delta(\delta)(M_\lambda - L_{\min})(1 - \Delta(\delta)) \\ &= 0. \end{aligned}$$

\square

Proof of Theorem 1

Let $\alpha \in (0, 1)$. Define

$$\begin{aligned} \tilde{M}_\lambda &= \frac{\mathcal{L}(\theta') + M_\lambda}{2} < M_\lambda, \\ \tilde{C} &= \{\theta \in B \mid \mathcal{L}_\lambda(\theta) \leq \tilde{M}_\lambda\}. \end{aligned}$$

By Assumption I, \mathcal{L}_λ is continuous so $Vol(\tilde{C}) > 0$. Then $\exists \delta > \delta_{\min}$ such that

$$\frac{Vol(B \setminus \tilde{C})}{(1 - \alpha)Vol(\tilde{C})} < e^{(M_\lambda - \tilde{M}_\lambda)\delta}.$$

We want to show that

$$\frac{\int_C e^{-\delta(\mathcal{L}_\lambda(\theta) - L_{\min})} d\theta}{\int_B e^{-\delta(\mathcal{L}_\lambda(\theta) - L_{\min})} d\theta} > \alpha \iff (1 - \alpha) \int_C e^{-\delta(\mathcal{L}_\lambda(\theta) - L_{\min})} d\theta > \alpha \int_{B \setminus C} e^{-\delta(\mathcal{L}_\lambda(\theta) - L_{\min})} d\theta.$$

It is enough to show

$$\int_{B \setminus C} e^{-\delta(\mathcal{L}_\lambda(\theta) - L_{\min})} d\theta < (1 - \alpha) \int_C e^{-\delta(\mathcal{L}_\lambda(\theta) - L_{\min})} d\theta.$$

If $\theta \in B \setminus C$, then

$$\mathcal{L}_\lambda(\theta) > M_\lambda \implies e^{-\delta(\mathcal{L}_\lambda(\theta) - L_{\min})} \leq e^{-\delta(M_\lambda - L_{\min})};$$

hence it is enough to show that

$$e^{-\delta(M_\lambda - L_{\min})} \text{Vol}(B \setminus C) < (1 - \alpha) \int_C e^{-\delta(\mathcal{L}_\lambda(\theta) - L_{\min})} d\theta.$$

Since the exponential is nonnegative and $\alpha \in (0, 1)$, it is equivalent to show

$$\frac{\text{Vol}(B \setminus C)}{1 - \alpha} < \int_{\tilde{C}} e^{-\delta(\mathcal{L}_\lambda(\theta) - M_\lambda)} d\theta.$$

If $\theta \in \tilde{C}$, then

$$\mathcal{L}_\lambda(\theta) \leq \tilde{M}_\lambda \implies \int_{\tilde{C}} e^{-\delta(\mathcal{L}_\lambda(\theta) - M_\lambda)} d\theta \geq \int_{\tilde{C}} e^{-\delta(\tilde{M}_\lambda - M_\lambda)} \theta = e^{-\delta(\tilde{M}_\lambda - M_\lambda)} \text{Vol}(\tilde{C}).$$

But

$$\frac{\text{Vol}(B \setminus C)}{(1 - \alpha) \text{Vol}(\tilde{C})} < e^{(M_\lambda - \tilde{M}_\lambda)\delta}$$

by our construction of δ .

□

Proof of Corollary 1

Since B is bounded, $e^{-\delta\mathcal{L}_\lambda(\theta)} \in L^1(B) \forall \delta \in \mathbb{R}$. Mimicking the argument of Proposition 1, Δ is differentiable and hence continuous at δ_{\min} . Since $\alpha \in (0, 1)$, Theorem 1 gives $\exists \delta > \delta_{\min}$ such that $\Delta(\delta_{\min}) < \alpha < \Delta(\delta)$. Then existence holds by the intermediate value theorem. Uniqueness follows from Proposition 2.

□

Proof of Theorem 2

Let

$$U(\delta) = \int_B |\theta_k| e^{-\delta(\mathcal{L}_\lambda(\theta) - L_{\min})} d\theta$$

$$V(\delta) = \int_B \left| \frac{\partial \mathcal{L}}{\partial \theta_k}(\theta) \right| e^{-\delta(\mathcal{L}_\lambda(\theta) - L_{\min})} d\theta$$

and

$$W(\delta) = \int_B e^{-\delta(\mathcal{L}_\lambda(\theta) - L_{\min})} d\theta.$$

Then we have

$$F_k(\delta) = \frac{U(\delta)}{W(\delta)} \frac{V(\delta)}{W(\delta)}.$$

Note that $W(\delta) > 0 \ \forall \delta > 0$, so it is enough to show that U , V , and W are differentiable. Theorem 6.28 in [38] gives the result using

$$|\theta_k| (\mathcal{L}_\lambda(\theta) - L_{\min}) e^{-\delta_{\min}(\mathcal{L}_\lambda(\theta) - L_{\min})},$$

$$\left| \frac{\partial \mathcal{L}}{\partial \theta_k}(\theta) \right| (\mathcal{L}_\lambda(\theta) - L_{\min}) e^{-\delta_{\min}(\mathcal{L}_\lambda(\theta) - L_{\min})},$$

and

$$(\mathcal{L}_\lambda(\theta) - L_{\min}) e^{-\delta_{\min}(\mathcal{L}_\lambda(\theta) - L_{\min})}$$

to dominate the derivatives of the integrands of U , V , and W , respectively. Applying Theorem 6.28 in [38] to $U(\delta)$, $V(\delta)$, and $W(\delta)$ yields

$$U'(\delta) = - \int_B |\theta_k| (\mathcal{L}_\lambda(\theta) - L_{\min}) e^{-\delta(\mathcal{L}_\lambda(\theta) - L_{\min})} d\theta$$

$$V'(\delta) = - \int_B \left| \frac{\partial \mathcal{L}}{\partial \theta_k}(\theta) \right| (\mathcal{L}_\lambda(\theta) - L_{\min}) e^{-\delta(\mathcal{L}_\lambda(\theta) - L_{\min})} d\theta$$

and

$$W'(\delta) = - \int_B (\mathcal{L}_\lambda(\theta) - L_{\min}) e^{-\delta(\mathcal{L}_\lambda(\theta) - L_{\min})} d\theta.$$

An application of the product and quotient rules to F_k yields

$$F'_k(\delta) = \left(\frac{U'(\delta)}{W(\delta)} - \frac{W'(\delta)}{W(\delta)} \frac{U(\delta)}{W(\delta)} \right) \frac{V(\delta)}{W(\delta)} + \left(\frac{V'(\delta)}{W(\delta)} - \frac{W'(\delta)}{W(\delta)} \frac{V(\delta)}{W(\delta)} \right) \frac{U(\delta)}{W(\delta)}.$$

Basic algebra along with the fact that $\frac{e^{-\delta(\mathcal{L}_\lambda(\theta) - L_{\min})}}{W(\delta)} = p(\theta)$ yields the result. □

References

References

- [1] A. Saltelli, M. Ratto, T. Andres, F. Campolongo, J. Cariboni, D. Gatelli, M. Saisana, and S. Tarantola. *Global Sensitivity Analysis: The Primer*. Wiley, 2008.
- [2] I.M. Sobol'. Global sensitivity indices for nonlinear mathematical models and their Monte Carlo estimates. *Mathematics and Computers in Simulation*, 55:271–280, 2001.
- [3] I.M. Sobol'. Sensitivity estimates for non linear mathematical models. *Math. Mod. Comp. Exp.*, 1:407–414, 1993.
- [4] Andea Saltelli. Making best use of model evaluations to compute sensitivity indices. *Computer Physics Communications*, 145(2):280–297, 2002.
- [5] M. Lamboni, B. Iooss, A.-L. Popelin, and F. Gamboa. Derivative-based global sensitivity measures: General links with Sobol' indices and numerical tests. *Mathematics and Computers in Simulation*, 87:45–54, 2013.
- [6] I. Sobol' and S. Kucherenko. Derivative based global sensitivity measures and the link with global sensitivity indices. *Math. Comp. Simul.*, 79:3009–3017, 2009.
- [7] I. Sobol' and S. Kucherenko. A new derivative based importance criterion for groups of variables and its link with the global sensitivity indices. *Comput. Phys. Comm.*, 181:1212–1217, 2010.
- [8] S. Kucherenko and B. Iooss. *Derivative based global sensitivity measures in: Handbook of Uncertainty Quantification*, pages 1241–1263. Springer, 2016.
- [9] Max D. Morris. Factorial sampling plans for preliminary computational experiments. *Technometrics*, 33(2):161–174, 1991.
- [10] B. Iooss and P. Lemaître. A review on global analysis methods. In G. Dellino and C. Meloni, editors, *Uncertainty Management in Simulation-Optimization of Complex Systems*, pages 101–122. Springer, 2015.
- [11] J. Bessac, E. M. Constantinescu, and M. Anitescu. Stochastic simulation of predictive space-time scenarios of wind speed using observations and physical models. *arXiv preprint arXiv:1511.09416*, 2016.
- [12] Chonggang Xu and George Zdzislaw Gertner. Uncertainty and sensitivity analysis for models with correlated parameters. *Reliability Eng. Sys. Safety*, 93(10):1563–1573, 2008.
- [13] C. Xu and G. Gertner. Extending a global sensitivity analysis technique to models with correlated parameters. *Computational Statistics and Data Analysis*, 51:5579–5590, 2007.

- [14] Genyuan Li, Herschel Rabitz, Paul E. Yelvington, Oluwayemisi O. Oluwole, Fred Bacon, Charles E. Kolb, and Jacqueline Schoendorf. Global sensitivity analysis for systems with independent and/or correlated inputs. *J. Phys. Chem.*, 114(19):6022–6032, 2010.
- [15] T. Mara and S. Tarantola. Variance-based sensitivity analysis of computer models with dependent inputs. *Reliability Eng. Sys. Safety*, 107:115–121, 2012.
- [16] Gaelle Chastaing, Fabrice Gamboa, and Clémentine Prieur. Generalized Hoeffding-Sobol decomposition for dependent variables-application to sensitivity analysis. *Electronic Journal of Statistics*, 2012.
- [17] Gaelle Chastaing, Clémentine Prieur, and Fabrice Gamboa. Generalized Sobol sensitivity indices for dependent variables: numerical methods. *Journal of Statistical Computation and Simulation*, pages 1–28, 2014.
- [18] Emanuele Borgonovo, William Castaings, and Stefano Tarantola. Moment independent importance measures: New results and analytical test cases. *Risk Analysis*, 31(3):404–428, 2011.
- [19] Changcong Zhou, Zhenzhou Lu, Luyi Li, Jun Feng, and Bintuan Wang. A new algorithm for variance based importance analysis of models with correlated inputs. *Applied Mathematical Modelling*, 37:864–875, 2013.
- [20] E. Borgonovo. A new uncertainty importance measure. *Reliability Eng. Sys. Safety*, 92:771–784, 2007.
- [21] Eunhye Song, Barry L. Nelson, and Jeremy Staum. Shapley effects for global sensitivity analysis: Theory and computation. *SIAM/ASA J. Uncertain. Quantif.*, 4:1060–1083, 2016.
- [22] J.H. Hart, A. Alexanderian, and P.A. Gremaud. Efficient computation of Sobol' indices for stochastic models. *SIAM J. Sci. Comput.*, 39(4):A1514–A1530, 2017.
- [23] Fabrice Gamboa, Alexandre Janon, Thierry Klein, and Agnés Lagnoux. Sensitivity analysis for multidimensional and functional outputs. *Electronic Journal of Statistics*, 8:575–603, 2014.
- [24] Ross Kindermann and J. Laurie Snell. *Markov Random Fields and Their Applications*, volume 1 of *Contemporary Mathematics*. AMS, 1980.
- [25] P. Sherlock, C. and Fearnhead and G. Roberts. The random walk metropolis: Linking theory and practice through a case study. *Statistical Science*, 25(2):172–190, 2010.
- [26] Jeffrey S. Rosenthal. *Optimal Proposal Distributions and Adaptive MCMC*, chapter 4, pages 93–112. Chapman and Hall/CRC, 2011.
- [27] M. Vihola. Robust adaptive metropolis algorithm with coerced acceptance rate. *Statistics and Computing*, 22(5):997–1008, 2011.

- [28] C. J. Geyer and E. A. Thompson. Annealing Markov Chain Monte Carlo with applications to ancestral inference. *Journal of the American Statistical Association*, 90(431):909–920, 1995.
- [29] C. J. Geyer. *Importance Sampling, Simulated Tempering, and Umbrella Sampling*, chapter 11, pages 295–312. Chapman and Hall/CRC, 2011.
- [30] Heikki Haario, Marko Laine, Antonietta Mira, and Eero Saksman. DRAM: Efficient adaptive MCMC. *Statistics and Computing*, 16:339–354, 2006.
- [31] M. K. Cowles and B. P. Carlin. Markov chain monte carlo convergence diagnostics: A comparative review. *Journal of the American Statistical Association*, 91(434), 1996.
- [32] Stephen P. Brooks and Gareth O. Roberts. Assessing convergence of markov chain monte carlo algorithms. *Statistics and Computing*, 8:319–335, 1997.
- [33] C. J. Geyer. *Introduction to Markov Chain Monte Carlo*, chapter 1, pages 3–48. Chapman and Hall/CRC, 2011.
- [34] S. P. Brooks and A. Gelman. General methods for monitoring convergence of iterative simulations. *Journal of Computational and Graphical Statistics*, 7(4):434–455, 1998.
- [35] C.T. Kelley. *Iterative Methods for Linear and Nonlinear Equations*. SIAM, 1995.
- [36] Tilmann Gneiting, Larissa I. Stanberry, Eric P. Grimit, Leonhard Held, and Nicholas A. Johnson. Assessing probabilistic forecasts of multivariate quantities, with an application to ensemble predictions of surface winds. *TEST*, 17(2):211–235, 2008.
- [37] Pierre Pinson and Robin Girard. Evaluating the quality of scenarios of short-term wind power generation. *Applied Energy*, 96:12–20, 2012.
- [38] Achim Klenke. *Probability Theory: A Comprehensive Course*. Universitext. Springer, 2 edition, 2014.

The submitted manuscript has been created by UChicago Argonne, LLC, Operator of Argonne National Laboratory (Argonne). Argonne, a U.S. Department of Energy Office of Science laboratory, is operated under Contract No. DE-AC02-06CH11357. The U.S. Government retains for itself, and others acting on its behalf, a paid-up nonexclusive, irrevocable worldwide license in said article to reproduce, prepare derivative works, distribute copies to the public, and perform publicly and display publicly, by or on behalf of the Government. The Department of Energy will provide public access to these results of federally sponsored research in accordance with the DOE Public Access Plan. <http://energy.gov/downloads/doe-public-access-plan>.